nature communications

Article

https://doi.org/10.1038/s41467-025-59848-2

Additive manufacturing of carbon fiber-reinforced thermoset composites via in-situ thermal curing

Received: 29 September 2023

Accepted: 7 May 2025

Published online: 20 May 2025

Check for updates

Carter F. Dojan[1,4], Morteza Ziaee[2,4], Alireza Masoumipour[2], Samuel J. Radosevich[2] & Mostafa Yourdkhani[1,2,3]

Fiber-reinforced polymer composites are lightweight structural materials widely used in the transportation and energy industries. Current approaches for the manufacture of composites require expensive tooling and long, energy-intensive processing, resulting in a high cost of manufacturing, limited design complexity, and low fabrication rates. Here, we report rapid, scalable, and energy-efficient additive manufacturing of fiber-reinforced thermoset composites, while eliminating the need for tooling or molds. Use of a thermo-responsive thermoset resin as the matrix of composites and localized, remote heating of carbon fiber reinforcements via photothermal conversion enables rapid, in-situ curing of composites without further post-processing. Rapid curing and phase transformation of the matrix thermoset, from a liquid or viscous resin to a rigid polymer, immediately upon deposition by a robotic platform, allows for the high-fidelity, freeform manufacturing of discontinuous and continuous fiber-reinforced composites without using sacrificial support materials. This method is applicable to a variety of industries and will enable rapid and scalable manufacture of composite parts and tooling as well as on-demand repair of composite structures.

Despite the increasing use of fiber-reinforced polymer composites (FRPCs) across multiple industries for the development of lightweight structures, the conventional manufacturing methods for composites still remain lengthy, inflexible, labor-intensive, energy-inefficient, and cost-prohibitive[1–3]. A major drawback of present composite manufacturing methods is the need for complex tooling for every new part design, which can take up to several months to produce based on traditional manufacturing and can account for more than 30% of the final product cost[4,5]. In addition, it might be quite challenging, or even impossible, to develop tooling for the manufacture of composite structures with complex geometries[6,7]. Production of a composite part using the developed tooling will then involve sustained, bulk heating of the material (and tooling) for several hours until the matrix thermoset resin of the composite is cured, leading to slow and energy-intensive manufacturing processes. Additive manufacturing (AM), also known as 3D printing, is promising for addressing the inefficiencies associated with conventional composite manufacturing and enabling rapid, flexible, and cost-effective custom manufacturing of FRPC structures[6]. Additive manufacturing of FRPCs requires automated deposition or placement of fully integrated constituents along designated paths, accompanied by rapid phase transformations of the matrix polymer for high-fidelity fabrication of high-quality structures in the absence of tooling surfaces and at ambient conditions. Current methods for the AM of FRPCs, using discontinuous or continuous fibers, primarily rely on the melt processing of thermoplastic polymers or photopolymerization of thermoset resins as the matrix polymer of composites[8–15]. While the AM of thermoplastic-matrix composites has garnered attention for its ease of processing and potential

[1]School of Materials Science and Engineering, Colorado State University, Fort Collins, CO, USA. [2]Department of Mechanical Engineering, Colorado State University, Fort Collins, CO, USA. [3]School of Manufacturing Systems and Networks, Arizona State University, Mesa, AZ, USA. [4]These authors contributed equally: Carter F. Dojan, Morteza Ziaee. e-mail: mostafa.yourdkhani@asu.edu

recyclability, most of the thermoplastic polymers employed in AM are unsuitable for structural applications, mainly due to their limited mechanical properties, thermal stability, and creep resistance[16,17]. In addition, the high melt-viscosity of thermoplastics presents a challenge in creating composites with a high concentration of fiber reinforcements (>50 vol%) while maintaining a low void content (<2 vol%), restricting the performance of produced composites[18–21]. In contrast, photocurable thermoset resins with substantially lower viscosities facilitate the AM of composites containing a high volume-fraction of fiber reinforcements. However, the low penetration depth of the incident light (ultraviolet or visible) caused by the screening effect of nontransparent fillers or reinforcements leads to partial and nonuniform curing of the matrix resin, limiting the print fidelity and printing speed and requiring hours of post-curing at elevated temperatures in size-limiting ovens[22–28]. While thermally curable thermosets, like those used in traditional composites, are ideal polymers for the AM of FRPCs, adoption of such resins in AM technologies has been hindered by their long cure cycles and flow-induced instabilities during high-temperature curing processes[29–32]. Direct ink writing (DIW) of highly thixotropic inks or reactive extrusion of thermoset resins reinforced by discontinuous fibers have been previously used to mitigate the processing issues of thermoset resins[8,33,34]. These approaches, however, are mostly suitable for manufacturing simple 2D geometries and cannot easily be used with continuous fibers. Additive manufacturing of continuous fiber-reinforced thermoset composites has been demonstrated by capillary-driven impregnation of fibers and in-situ thermal curing via Joule heating[35]. This approach similarly produces low-fidelity composite parts with a simple geometry, cannot be applied to the AM of discontinuous FRPCs, and has limited processability and printing speeds due to the requisite wicking effect. Frontal polymerization (FP) has been recently introduced as a promising curing strategy for 3D printing of discontinuous and continuous fiber-reinforced composites by in-situ curing of the matrix thermoset resin through a self-propagating chemical reaction[36–39]. While the self-sustaining, FP-assisted 3D printing is promising for freeform manufacturing of composite structures, its practical application is limited by the low front velocities of the FP chemistries (<10 cm min^{-1}), reaction quenching caused by heat losses through boundaries, and difficulties in maintaining a high frontal reactivity in the presence of a high concentration of fillers or reinforcements[36,40–42]. It is thus desirable to develop robust AM techniques for the high-quality manufacture of thermoset-matrix composites for use in aerospace, space, marine, energy, automotive, and biomedical applications.

Here, we present an AM method for rapid, tool-free production of high-quality thermoset-matrix composites by in-situ, immediate thermal curing of composite materials. Use of a rapid-curable, thermoresponsive thermoset resin along with a local photothermal stimulus mounted on the printhead of a robotic platform allows for on-demand rigidization of carbon fiber composites on existing surfaces or in midair. By tuning the cure kinetics and rheological profiles of the resin system, we demonstrate the AM of FRPCs using both discontinuous and continuous carbon fibers. Systematic experimental studies are performed to understand the effect of various processing parameters on the printability of the composite materials and guide the design of reliable AM processes. This method offers rapid, scalable, and resource-efficient custom manufacturing of custom FRPC structures while eliminating the need for tooling and post-curing steps, and can be applied to a variety of rapid-curable polymer resins, reinforcement types, and thermal stimuli.

Results and Discussion

Additive manufacturing of composites via in-situ photothermal-assisted curing

Our approach for the AM of FRPCs is predicated on the use of rapid-curable, thermoresponsive thermoset resins as the matrix phase of composites coupled with local heating of the composite material immediately upon deposition by a robotic platform (Fig. 1a). Here, the ring opening metathesis polymerization (ROMP) of dicyclopentadiene (DCPD) in the presence of a second-generation Grubbs' catalyst and phosphite inhibitor (Fig. 1b) is used to develop thermoresponsive

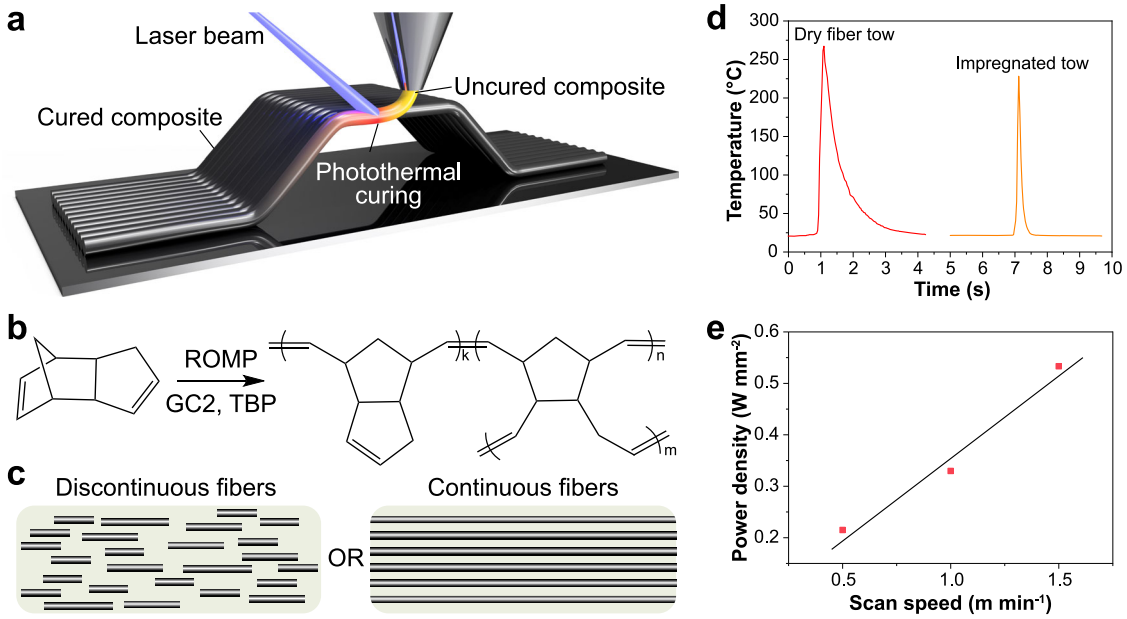

Fig. 1 | Additive manufacturing of composites via photothermal-assisted curing of thermoresponsive resins. a Schematic representation of the additive manufacturing process. Localized photothermal heating of the composite material immediately upon deposition by a robotic platform allows for high-fidelity printing of composites on solid substrates and in midair. **b** Scheme of the ROMP of the thermoresponsive DCPD resin system using a second-generation Grubbs' catalyst (GC2) and tributyl phosphite inhibitor (TBP). **c** The tunable viscosity and cure kinetics of DCPD resin enables additive manufacturing of composites using discontinuous and continuous carbon fibers. **d** Photothermal response of dry and resin-impregnated carbon fiber tows (tow size = 3000) as the laser beam passes a point of interest on the fiber tow at a scanning rate of 1.5 m min^{-1}. **e** Laser power density should be adjusted when decreasing the printing speed or using various tow sizes.

resins for composite AM. The tunable viscosity of this resin system, ranging from a low-viscosity liquid resin to a viscous gel, is ideal for developing new processing methods for the AM of both discontinuous and continuous fiber-reinforced thermoset composites (Fig. 1c). The resulting polymer, polydicyclopentadiene (pDCPD), is a high-performance crosslinked thermoset with a good combination of high modulus and strength, thermal stability, impact resistance, fracture toughness, and chemical resistance while having a low density, cure shrinkage, and moisture absorption[43–46]. These attributes make pDCPD an ideal polymer for use in structural applications.

On-demand, in-situ curing and phase transformation of the matrix resin in high-fidelity AM of FRPCs requires rapid, localized heating of the deposited material during the printing process. While a variety of external energy sources can be used to supply the requisite thermal energy for composite curing, we use photothermal conversion for controlled, energy-efficient heating and curing of the deposited material at high heating rates. Photothermal conversion has recently been demonstrated for localized initiation of frontal polymerization using carbon particles[47,48]; however, these approaches either exhibited low heating rates (initiation reaction times >10 s) when a high-power (output power = 25 W), wide-spectrum light source was used or required a complex, expensive laser system (titanium:sapphire laser), rendering their use in AM processes impractical. For efficient photothermal energy conversion, the good absorption property of carbon fibers[49] is exploited here to convert the energy of an incident monochromic blue laser light (wavelength = 450 nm) to heat within a local zone within 100–200 ms (Fig. 1d). The laser diode used in this study is compact, low power (4.5 W), and inexpensive, making it suitable for integration on robotic systems and continuous, rapid heating of composite materials during printing. The generated heat then rapidly increases the temperature of the surrounding resin through conduction by leveraging the high thermal conductivity of carbon fibers. Previous studies on the frontal curing of the DCPD resin system indicate that it rapidly and fully cures at temperatures ranging from 200 °C to 240 °C[50,51]. For effective heating of carbon fiber composite filaments, we aim to increase the temperature of the composite filament to ~220–240 °C by tuning the laser parameters (i.e., power density, scan speed) while ensuring that the entire width of the filament is covered by the laser beam. Printing studies with a resin-impregnated continuous carbon fiber filament (tow size = 3000) using the 4.5 W blue laser diode (power density = 0.53 W mm^{-2}) reveals that the maximum scanning speed for achieving the target cure temperature is ~1.5 m min^{-1} (Fig. 1d, e). The reduction in the peak temperature of the photothermal profile of the resin-impregnated fibers compared with dry fibers in Fig. 1d is attributed to the increased thermal mass and heat absorption by the matrix resin. Heating larger diameter carbon fiber filaments requires increasing the projected diameter of the beam, thus decreasing the laser power density and necessitating lower scan speeds to reach the same target temperature. The observed linear relationship between power density and scan rate for reaching the target cure temperature (Fig. 1e) provides a valuable insight for scaling the appropriate printing speed for curing composite filaments of various sizes. Thus, higher heating rates and allowable scanning (printing) speeds can be expected using a laser source with a higher output power.

The integration of the thermoresponsive DCPD thermoset resin with the rapid photothermal heating of carbon fibers in the AM process enables unprecedented manufacturing of discontinuous and continuous carbon fiber-reinforced composites and addresses shortcomings of the conventional manufacturing methods and commercial AM processes.

Additive manufacturing of discontinuous carbon fiber-reinforced composites

We primarily focus on the AM of discontinuous carbon fiber-reinforced composites to demonstrate the ability to in-situ cure and rigidize the matrix polymer resin and assess its cure behavior and properties under various printing conditions. Unlike continuous FRPCs, in discontinuous FRPCs fibers do not provide the composite with continuous mechanical integrity, facilitating the study of polymer properties and the effect of the resin cure behavior on print quality and composite performance. In the AM of discontinuous carbon FRPCs, we use DIW to extrude composite inks through a printing nozzle, followed by in-situ curing of the ink via photothermal conversion (Fig. 2a, b). Printable inks with a shear-thinning behavior for easy flow through fine printing nozzles are prepared by staging and partially curing the DCPD resin to create a viscoelastic gel[36,52] and adding 15 vol% of milled carbon fibers (unless otherwise specified) (Fig. 2d). Maintaining the ink temperature at −5 °C during printing minimizes the background polymerization of the ink and facilitates access to an extended processing window with a relatively constant ink viscosity for a reliable, reproducible printing process (Fig. S1). Rapid photothermal heating and curing of the composite ink via a laser source mounted on a robotic platform allows for freeform printing of overhanging composite filaments at high printing speeds (up to 1.5 m min^{-1}), while eliminating the need for support materials commonly used in AM processes (Fig. 2a). Thermal infrared imaging of the printing process demonstrates the rapid increase in the temperature of the composite ink at the focused laser spot (Fig. 2b). Optical micrograph in Fig. 2c exhibits the void-free and highly circular cross-section of a printed composite filament.

We examine the effect of various processing parameters on the printability of the composite material by printing straight filaments and measuring the degree-of-cure of the resulting composites using differential scanning calorimetry (DSC). Filaments printed using nozzles with an inner diameter, D_i, ranging from 0.6 mm to 1.6 mm exhibit a similar, high degree of cure (ranging from 96% to 98%), indicating successful, rapid heating and curing of filaments of various sizes at high printing speeds (i.e., 1.5 m min^{-1}) (Fig. 2e). Slightly higher degrees of cure can be achieved by reducing the printing speed while commensurately decreasing the laser power density (Fig. 2f). At lower printing speeds, the generated heat is transferred more evenly across the cross-section of the filament, resulting in a more uniform curing. In contrast, increasing the print speed to 2 m min^{-1} and higher results in insufficient heating and low cure temperatures using this particular laser source, preventing the rapid cure of the composite material. We surmise that higher printing speeds can be achieved using laser sources with a higher output power or a spatially aligned array of multiple laser sources. Our experimental studies also reveal that the concentration of carbon fibers does not significantly affect the photothermal conversion and cure rate of composite inks (Fig. 2g). Decreasing the carbon fiber content from 15 vol% to 5 vol% has a minimal impact on the degree of cure in the printed composites, suggesting that carbon fibers can effectively convert the incident electromagnetic energy and transfer the generated heat within the filament at various concentrations. In the absence of carbon fibers, the neat DCPD ink does not heat in response to the incident laser beam, leading to unsuccessful printing (Movie S1). The insights gained from these experimental studies are used to 3D print various composite structures based on freeform (unsupported) (Fig. 2h, i) or layer-by-layer (Fig. 2j) printing strategies on a room-temperature glass substrate. These parts are printed using a single continuous print path, without any interruptions in the printing process. Following the printing, the composite parts are fully cured and do not need any post-curing steps (Movie S2). The bracket structure in Fig. 2k illustrates an example part printed using a combination of the two strategies, where the first layer, consisting of four adjacent paths is first printed using the freeform printing strategy and then the second layer is printed on top of the first layer, serving as a support (Movie S3). This structure is printed in 100 s using only 0.45 kJ of thermal energy, reducing the curing energy by more than four orders of magnitude compared to the traditional, oven curing of a similar part made of an epoxy-based composite (estimated energy consumption of 6912 kJ based on a 6 h

https://doi.org/10.1038/s41467-025-59848-2

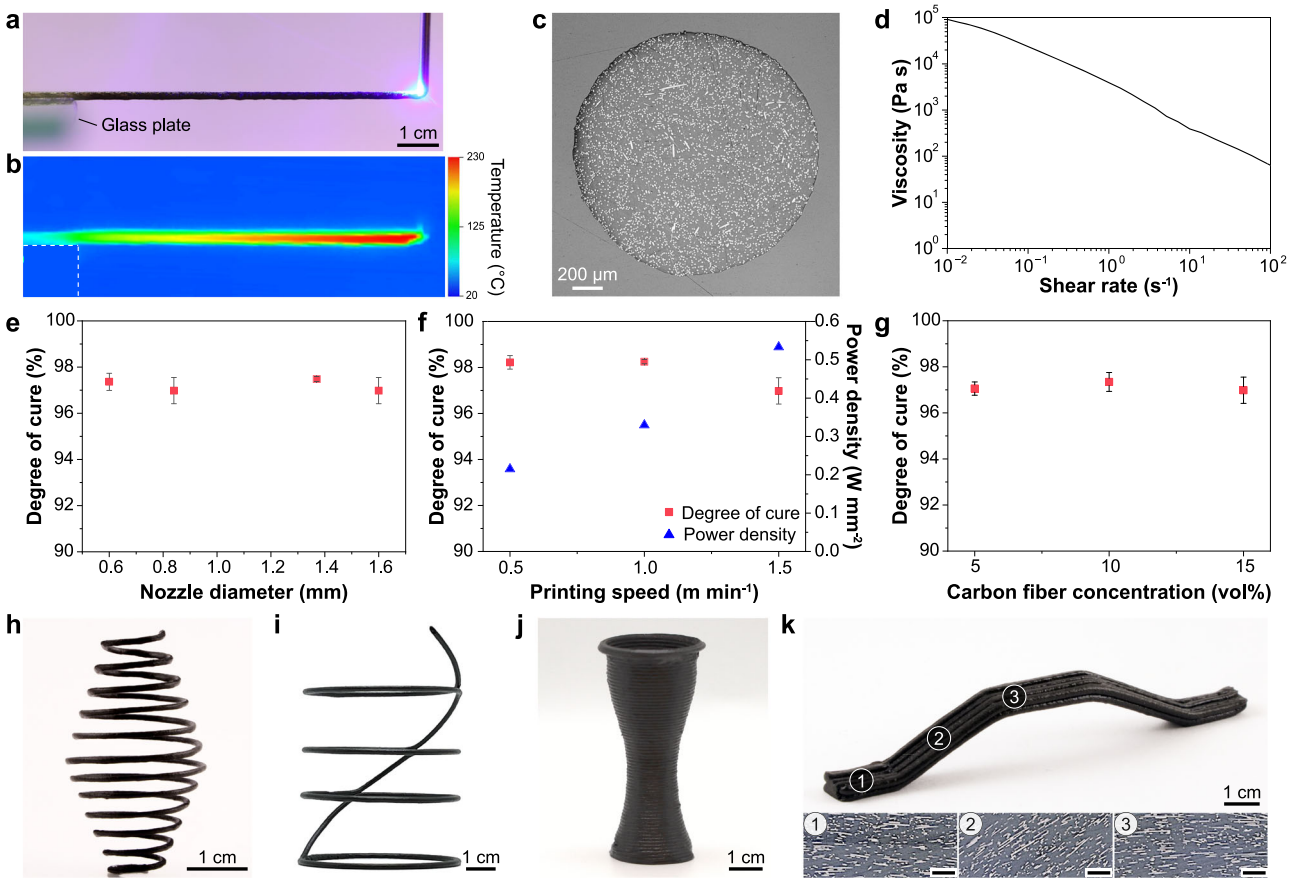

Fig. 2 | Additive manufacturing of discontinuous fiber-reinforced composites. **a**, **b** Digital and infrared thermal images, respectively, from freeform printing of a composite filament (printing speed = 1.5 m min^{-1}). The linearity of this filament is estimated by calculating the root mean square deviation, RMSD, from the planned straight line as 0.028 mm over the overhang length. **c** Optical micrograph from the cross-section of the filament printed in a. The cross-section exhibits a circularity of 95.7%. **d** Shear-thinning behavior of the composite ink containing 15 vol% of carbon fibers. **e** Degree of cure of filaments printed using various nozzle diameters at a printing speed of 1.5 m min^{-1}. **f** Degree of cure of filaments printed at various printing speeds using a nozzle with an inner diameter, D_i, of 1.6 mm. **g** Degree of cure of filaments printed with inks containing various concentrations of carbon fiber. Error bars in e-g represent standard deviation from the mean ($n = 2$). **h**–**k** Examples of composite parts printed using freeform and/or layer-by-layer printing strategies at a printing speed of 0.5 m min^{-1} and using a nozzle with an inner diameter of 1.6 mm. Images ①-③ in **k** show the fiber orientation in three regions of the printed part. Scale bars represent 200 μm.

cure cycle in a small, laboratory-scale convection oven with an inner volume of 66 L and energy consumption of 0.32 kW at 150 °C). Furthermore, continuous deposition of the composite ink along 3D printing paths allows for orienting fibers along the filament length in 3D space (images ①-③ in Fig. 2k), providing out-of-plane fiber orientation and 3D reinforcement in the printed structure. It is worth noting that in conventional AM methods, fiber orientation is predominantly restricted to a two-dimensional (2D) configuration, as materials are typically deposited layer-by-layer, inherently constraining the orientation and reinforcement capabilities of fibers within the printed layers[53,54].

The mechanical performance of the additively manufactured composites is evaluated by performing flexural tests on beam specimens printed with print paths either parallel or transverse to the longitudinal axis of the beam. For comparison, three control samples are also prepared and tested similarly. The control cast sample is prepared by manually pouring the composite ink in a mold and bulk curing in an oven. Other control samples are prepared by printing (i.e., depositing) the composite ink directly in the mold either in parallel or transverse directions without in-situ curing, followed by transferring the mold to the oven for bulk curing. The flexural modulus and strength of the tested samples are compared in Fig. 3a. The samples printed parallel to the beam axis, whether cured in-situ or in oven, exhibit the highest flexural modulus and strength, which is attributed to the high alignment of carbon fibers along the printing direction and obtaining the maximum possible reinforcement. In contrast, the samples prepared by printing transverse to the beam axis exhibit inferior flexural properties compared to other samples, due to the orientation of fibers normal to the loading direction and lack of reinforcement from fibers along the beam axis. For both the parallel and transverse samples, the in-situ cured samples have comparable flexural modulus to control samples prepared by depositing ink into the mold and bulk curing in an oven; however, in-situ cured samples exhibit slightly lower flexural strength compared with oven-cured counterparts, indicating the effect of the interface formed during the printing process on the flexural strength of printed composites. The cast samples exhibit higher flexural strength and modulus than the transverse samples but lower than the parallel samples, due to the random orientation of discontinuous fibers compared to the aligned fibers in the in-situ and oven-cured printed samples. Short beam shear (SBS) tests are performed on samples printed parallel to the beam axis and cured in-situ or by oven to further evaluate the role of interfaces formed by curing in-situ. Comparable SBS strengths of 13.57 ± 1.47 MPa and 13.46 ± 0.50 MPa are obtained for oven- and in-situ-cured samples, respectively. However, the failure modes differed between the in-situ specimens, which failed in shear and/or tension, and the oven-cured samples, which failed only in tension, rendering the SBS analysis inconclusive. The absence of shear failure in oven-cured samples

https://doi.org/10.1038/s41467-025-59848-2

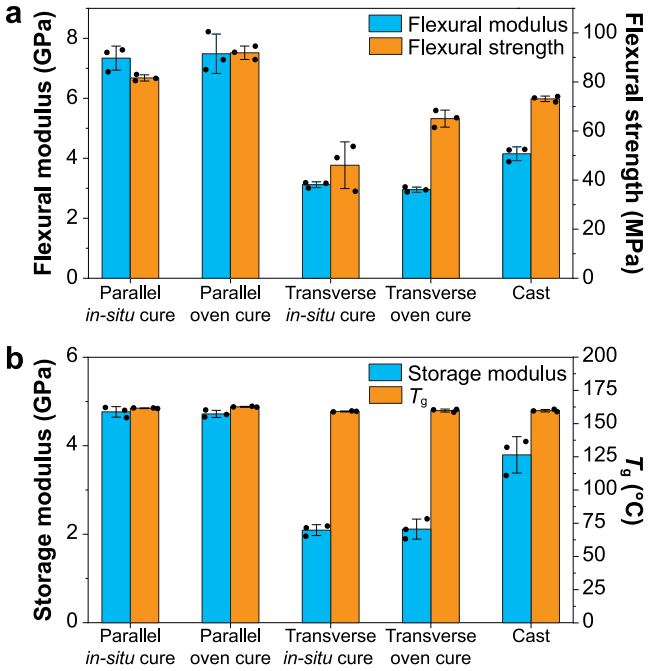

Fig. 3 | Characterization of discontinuous carbon FRPC samples. a Flexural modulus and strength of composite beams prepared by printing and in-situ curing the ink in parallel or transverse to the longitudinal axis of the beam. Three control samples are also considered. The cast sample is prepared by manually pouring the ink in a mold, followed by bulk curing in an oven. For the two other control samples, the ink is printed in the mold, in parallel or transverse to the beam axis, without in-situ curing; the mold is then transferred to the oven for bulk curing. All samples contain 15 vol% of discontinuous carbon fibers. Error bars represent standard deviation from the mean ($n = 3$). **b** Storage modulus and glass transition temperature, T_g, of printed and cast samples determined by dynamic mechanical analysis (DMA) measurements. Error bars represent standard deviation from the mean ($n = 3$).

supports the attribution of reduced flexural strength to layer interfaces in in-situ-cured samples. We believe improved flexural properties could be realized for in-situ-printed samples via ink modification, such as the addition of antioxidants or by forming interpenetrating polymer networks[32,55–57].

Dynamic mechanical analysis (DMA) measurements performed on prepared samples show similar viscoelastic behavior between in-situ and oven-cured samples (Fig. 3b). Samples prepared by depositing fibers parallel and transverse to the beam axis have the highest and lowest storage moduli, respectively, following a trend similar to the flexural testing results. In-situ and oven-cured samples behave similarly with comparable storage moduli, reinforcing the minimal impact of the curing method on the part modulus. Furthermore, all samples exhibit a similar glass transition temperature (T_g), ranging from 159.8 °C to 163.3 °C, determined from the peak of tan(δ) curves in DMA measurements, indicating successful curing and crosslinking of composite specimens using both in-situ and oven-curing approaches.

Additive manufacturing of continuous carbon fiber-reinforced composites

The ability to immediately in-situ cure the matrix thermoset resin of composites by photothermal conversion also enables the high-fidelity AM of continuous FRPCs containing a high concentration of carbon fiber reinforcement. For the AM of continuous FRPCs, the printing process is slightly modified to allow for controlled placement of uncured composite material along a given print path, followed by immediate photothermal curing and rigidization similar to the AM of discontinuous FRPCs. A continuous carbon fiber tow is impregnated with the resin on the printhead of a robotic platform, fed through a dispensing nozzle, and placed along the print path by adjusting the angle of the dispensing nozzle and/or using a compaction roller (Fig. 4a). The laser beam is focused on the fiber tow at a small distance (~3–5 mm) from the edge of the nozzle or roller to immediately cure the material and maintain the print geometry. Owing to the low, and relatively stable, viscosity of the resin system at room temperature (Fig. 4c), a high concentration of continuous fibers can be readily impregnated with the resin and fed thorough a nozzle with a slightly larger diameter than that of the impregnated tow. By tailoring the ratio of the fiber tow diameter to the inner diameter of the dispensing nozzle, we additively manufacture continuous FRPCs with high volume-fractions of carbon fibers, ranging from 50 vol% to 70 vol% (Fig 4b, S2). Additionally, the easy impregnation of fibers with resin and controlled compaction of the composite material results in composites with little to no void content (0 to 1.5 vol%), which is quite challenging to achieve using other composite AM methods.

In-situ thermal curing of continuous carbon FRPCs results in fully cured composites with degrees of cure exceeding 95% (Fig. 4d, e). Adjusting the laser power density based on the findings presented in Fig. 1e allows for high-speed printing of fully cured continuous carbon fiber composites, with speeds of up to 1.5 m min^{-1} (Fig. 4d). Additionally, our AM process can efficiently heat and cure composites with varying filament diameters by printing composite filaments with different tow sizes while adjusting the printing speed, laser spot size, and power density (Fig. 4e). Figure 4f depicts a high-aspect-ratio (aspect ratio = 750) composite beam printed in midair along a straight path, which can maintain its straight geometry with minimal deflection under self-weight, owing to its fully cured matrix and high fiber content.

In marked contrast with conventional AM approaches, our AM method does not require detailed control over the substrate or surrounding air temperature, facilitating the scalable manufacturing of composite structures. Multilayer continuous FRPC structures are easily printed on room-temperature glass substrates by automated placement and rapid photothermal curing of the impregnated fibers (Fig. 4g–i; Movie S4). Figure 4i shows an example part printed in a single step over 8 h. By contrast, manufacturing the same part using conventional methods would take several days or weeks and involve multiple processing steps, including fabrication of dissolvable tooling, manual layup and vacuum bagging of the composite material, curing the part in an autoclave or oven for several hours, removing the part from the layup, and dissolving the tooling in either aqueous or non-aqueous solvents. Therefore, our AM approach simplifies the manufacture of custom composite parts by reducing the manufacturing time, eliminating the need for multiple processing steps and consumables, and minimizing manual intervention, ultimately resulting in faster production and lower costs. In addition, controlling the placement and compaction of fibers allows for fabricating composites with minimal inter-tow void formation (Fig. S3). Tensile tests performed on unidirectional printed and control cast composite samples (fiber volume fraction, $V_f = 51.4\%$ for both samples) reveal similar mechanical performance, where a modulus of 106.7 ± 9.2 GPa and 110.7 ± 18.9 GPa and strength of 1.48 ± 0.10 GPa and 1.66 ± 0.15 GPa are obtained for printed and cast samples, respectively. Additional characterization through short beam shear (SBS) testing is required to fully evaluate the material's properties; however, further process development is needed to produce specimens that conform to ASTM standards for shear failure.

We also demonstrate freeform, out-of-plane AM of continuous FRPCs while maintaining the minimal void content in composites as the print path transitions from a solid substrate into air (Fig. 4j). Large-scale, freeform printing of composites between various surfaces is also enabled using a 6-axis robotic arm (Fig. 4k, Movie S5). After printing a straight path on a glass substrate, the printhead moves off the tool plate to reach another substrate positioned 50 cm horizontally and

https://doi.org/10.1038/s41467-025-59848-2

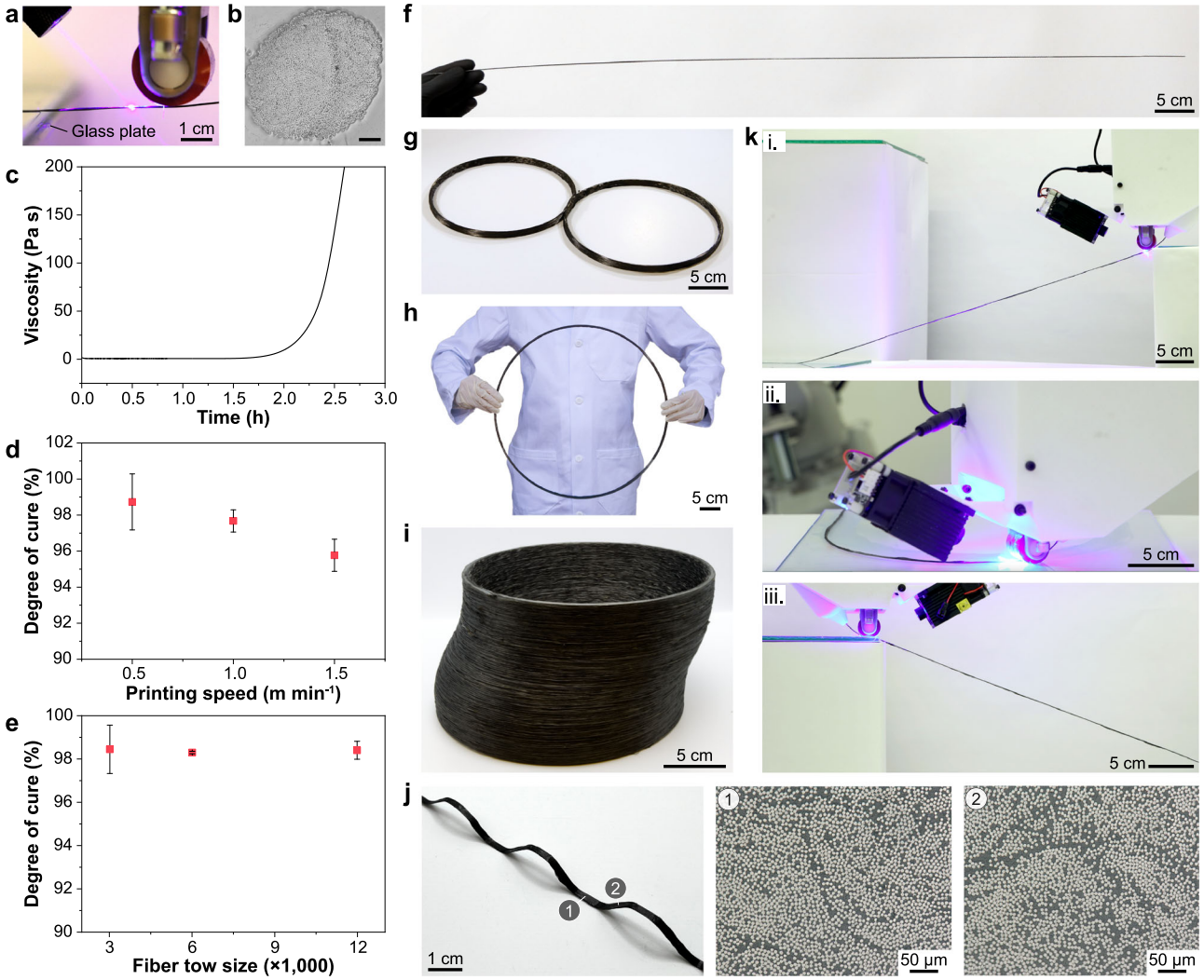

Fig. 4 | Additive manufacturing of continuous fiber-reinforced composites. **a** Curing a composite filament in midair upon placement by a roller. **b** Optical micrograph from the cross-section of a composite filament containing 70.8 vol% of carbon fibers placed in midair using the roller (circularity = 84.0%). The scale bar represents 100 μm. **c** Rheological measurement of the resin at room temperature, showing minimal change in viscosity within 2 h after the preparation of the resin. The initial viscosity of resin is 0.5 Pa s. **d** Degree of cure of composite filaments (tow size = 3000) printed at various speeds while adjusting the laser power density. **e** Degree of cure of composite filaments printed using various tow sizes (printing speed = 0.5 m min^{-1}). Error bars in d, e represent standard deviation from the mean ($n = 2$). **f** Image of a high-aspect-ratio (aspect ratio = 750) composite filament after printing, demonstrating its high stiffness and minimal deflection under self-weight. **g**–**i** Example composite parts manufactured using layer-by-layer printing and in-situ curing strategy. The parts in **g**, **h**, and **i** are made using 24, 24, and 100 layers of fiber tows in around 25 min, 30 min, and 8 h, respectively. **j** A composite part manufactured using the freeform printing strategy. The images in ① and ② depict the void-free cross-sections of the part in two different regions. **k** Printing a composite filament along a 1.8-m print path on various surfaces and in midair in 204 s.

20 cm vertically away from the original substrate (Fig. 4k(i.)). The printing process continues on the new substrate, following a curvilinear path (Fig. 4k(ii.)), and then proceeds to print another straight line in midair to reach a third substrate positioned at a similar distance (Fig. 4k(iii.)). This demonstration illustrates successful printing of continuous fiber composites along a continuous 1.8-meter path, including in-plane curvatures and non-planar angles, on various substrates and in midair in 204 s.

In summary, we have developed an additive manufacturing method for rapid, flexible, and energy-efficient fabrication of fiber-reinforced thermoset composites by synergistic integration of thermoresponsive thermoset resins and remote heating of carbon fibers enabled by photothermal conversion. We demonstrate freeform and layer-by-layer additive manufacture of both discontinuous and continuous fiber-reinforced thermoset composites without controlling the substrate and surrounding air temperatures, which are necessary in most AM techniques, while eliminating the need for further post-curing in an oven. Controlled placement and curing of composite materials using our AM approach allows for creating composites with up to 70 vol% of fibers and minimal void content (0-1.5 vol%) as well as out-of-plane 3D orientation of fibers without using any support materials, which is challenging to achieve using other AM or conventional processing techniques. We believe this approach is applicable to a wide variety of thermoresponsive resins, reinforcement scales (i.e., nanoscale reinforcements to continuous fibers), and reinforcement materials (e.g., aramid, glass, and basalt fibers) by selecting the appropriate electromagnetic radiation. As an example, AM of discontinuous aramid fiber composite is demonstrated in Fig. S4 using the same blue laser diode and printing setup. The manufacturing rates can be further increased by controlling the cure kinetics of the matrix resins as well as the efficiency and rate of energy conversion. We envision our additive manufacturing method will enable rapid and scalable manufacture of composite tooling and complex parts, repair of existing structures, and multimaterial printing of multiscale composites.

Methods

Materials

Dicyclopentadiene (DCPD), 5-ethylidene-2-norborene (ENB), and second-generation Grubbs catalyst (GC2) were purchased from Sigma Aldrich. Tributyl phosphite inhibiter (TBP) and phenylcyclohexane (PCH) were purchased from TCI America. Milled carbon fibers (PX30; average length = 72 µm) were kindly donated by Zoltek Corporation. Continuous carbon fibers were donated by Hexcel (AS4C fibers; tow size: 3000, 6000, and 12,000), Toray (T700S fibers; tow size: 12,000), and Zoltek Corporation (PX35 fibers; tow size: 50,000). All materials were used as received without further purification.

Photothermal heating measurements

The photothermal response of dry or resin-impregnated carbon fibers to the blue laser beam (output power = 4.5 W; wavelength = 450 nm) is determined by fixing a carbon fiber tow between two support blocks 10 cm apart and scanning the surface of the fiber tow by the laser mounted on a tabletop robotic platform (F5200N, Fisnar). The time-temperature profile of a fixed region of interest on the fiber tow is measured using an infrared thermal camera (FLIR T540). The power density of the laser beam on the fiber tow is adjusted by changing the projected spot size of the beam at the plane of the fiber tow and calculated by dividing the output power of the laser by the projected area.

Preparation of the DCPD resin system

The thermoresponsive DCPD resin system is prepared by first mixing DCPD with 5 wt% ENB at 50 °C for 1 h and degassing the solution overnight to suppress the melting point of DCPD and create a liquid resin at room temperature. All future references to the DCPD resin herein will refer to the 95:5 DCPD/ENB solution. For all sample preparations, 7.70 mg of GC2 and 2.38 µL of TBP are dissolved in 1 mL of PCH via sonication for 10 min, followed by mixing the resulting solution with 12 g of the DCPD resin.

AM of discontinuous FRPCs

To prepare the inks for DIW of discontinuous FRPCs, the DCPD resin solution is placed in an incubator oven pre-heated to 30 °C for 1 h to increase the resin viscosity. Unless otherwise specified, 15 vol% of milled carbon fibers is added to the staged resin and mixed using a planetary centrifugal mixer (AR-100, Thinky USA) for 5 min. The ink is again placed in the incubator at 30 °C for an additional 20 min to create a highly viscous ink suitable for DIW. The resulting ink is then transferred to a 10 mL syringe barrel and centrifuged for 5 min to remove any air bubbles. For the study of the effect of carbon fiber concentration on the degree of cure of printed composites, inks containing 5 and 10 vol% of milled carbon fibers are also prepared according to the same procedure. The control neat DCPD ink for assessing the photothermal response and curing of the ink in the absence of carbon fibers is prepared similarly without the final degassing step. Following the preparation of the printable inks, the syringe barrel containing the ink is placed inside an aluminum syringe holder mounted on the three-axis gantry robot (F5200N, Fisnar). The ink temperature is maintained at -5 °C using two thermoelectric Peltier coolers embedded inside the aluminum syringe holder to prevent the room-temperature crosslinking of the resin and retain the ink viscosity during the printing process. The ink is pneumatically dispensed through various nozzles (inner diameter, D_i = 0.6–1.6 mm) using a high-precision dispenser (DC100, Fisnar) under air pressures of 40–250 kPa and in-situ cured using the blue laser diode. For the AM of objects in Fig. 2h–j, the ink is extruded on a custom-designed rotating platform spinning at a constant speed of 6 rpm while moving the nozzle along x and z directions. The structures in Fig. 2h–k are printed using a printing speed of 0.5 m min^{-1}.

AM of continuous FRPCs

For the AM of continuous FRPCs, the freshly prepared DCPD resin without the staging steps (as described in Section 4.3) is used to exploit the low viscosity of the resin solution for easy impregnation of continuous fibers during the printing process. Unless otherwise specified, AS4C fibers from Hexcel are used in the AM of continuous FRPC parts. Continuous carbon fiber tows (tow size = 3000, 6000, or 12,000) are fed through a syringe barrel filled with 20 mL of the DCPD resin at room temperature and placed along a desired print path using a dispensing nozzle and/or compaction roller. As the printhead of the robotic platform moves along the print path, fibers are pulled through the syringe barrel and impregnated with the resin, and then locally cured via photothermal conversion after placement. Various nozzle sizes (D_i = 0.6-1.6 mm) are used based on the fiber tow size to control the fiber volume fraction of the printed composites. When printing on solid substrates, the compaction roller attached to a compression spring is used to apply 10 N of force on fibers to properly compact the material and minimize void formation; however, the use of the roller is not necessary when printing in midair. The composite parts in Fig. 4f, h, i, k, and Fig. 4g are printed using ABB IRB 4600 and Kuka KR 6 R900 six-axis robotic arms, respectively. The parts in Fig. 4h, i are printed on a robotic turntable working collaboratively with the ABB robotic arm. All other printing studies are carried out using the same tabletop gantry robot used in the AM of discontinuous FRPCs. The composite parts in Fig. 4f–h, k are printed using a tow size of 12,000, a needle (for controlling the fiber volume fraction) with an inner diameter of 1.04 mm, and a printing speed of 0.5 m min^{-1}. For printing the curved baffle part in Fig. 4i, fiber tows with a tow size of 50,000, needle diameter of 2.27 mm, and printing speed of 0.2 mm min^{-1} are used. The composite bracket part in Fig. 4j is printed using three tows of carbon fiber (total tow size = 36,000) fed through a custom nozzle with an inner dimensions of 5 mm × 1 mm at a print speed of 0.3 m min^{-1}. Where necessary, the surface adhesion of the glass substrate is enhanced by applying a thin layer of adhesive from a glue stick.

Rheological measurements

The rheological properties of the liquid resin and composite ink are determined using a Discovery HR-2 Rheometer (TA Instruments) with a 40 mm flat geometry and a gap size of 1000 µm. Steady-state flow experiments are conducted on the composite ink at a reference temperature of −5 °C at controlled shear rates ranging from 0.01 to 100 s^{-1} to measure the rheological response of the ink. Isothermal time-sweep measurements on the liquid resin and composite ink are performed at 25 °C and −5 °C respectively at a constant strain of 0.1% and frequency of 1 Hz.

Degree of cure measurements

The degree of cure of the composite samples prepared under various processing conditions are determined by differential scanning calorimetry (DSC) on a DSC 2500 machine (TA Instrument). Cured composite specimens (5–10 mg) are placed in aluminum hermetic pans, sealed, and heated from 25 to 250 °C at a heating rate of 5 °C min^{-1} to measure the residual heat of reaction (H_r). The total heat of reaction of the resin (H_T = 277.43 J/g) is also measured by performing DSC measurements on uncured ink specimens (2–3 mg) according to the same procedure. Representative heat flow curves for uncured resin and cured composite specimens are shown in Fig. S5. The degree of cure (α) of printed composites is calculated as,

$$\alpha = 1 - \frac{H_r}{H_T} \tag{1}$$

Mechanical testing of composites

Three-point flexural tests are conducted on the manufactured discontinuous fiber composite beam specimens using an Instron 5966

Universal Testing System equipped with a 10 kN force capacity transducer.

The flexural strength and modulus of printed and control samples are determined according to the ASTM D790 standard at ambient temperature, crosshead speed of 1.5 mm min^{-1}, and span length of 52 mm. Bar specimens with dimensions of 65 mm × 12 mm × 3 mm are prepared by printing and in-situ curing the composite ink (15 vol% carbon fibers) in parallel or transverse to the longitudinal axis of the beam using a nozzle with an inner diameter of 1.6 mm. Control samples with the same dimensions are also prepared by either printing (in parallel or transverse direction) or pouring the composite ink in a silicone mold, followed by curing in an oven at 170 °C for 1.5 h. The flexural strain, ε, on the outer surface of the test specimens at midspan is calculated as,

$$\varepsilon = \frac{6dD}{L^2} \tag{2}$$

where D is the crosshead displacement, d is the thickness of the beam, and L is the support span length. Flexural stress, σ, is calculated as,

$$\sigma = \frac{3PL}{2bd^2} \tag{3}$$

where P is the applied load at the center of the beam and b is the width of the beam. It is assumed that the beam fails at the midspan of the beam. Flexural modulus and strength are estimated as the slope of the flexural stress-strain curve and the maximum stress sustained by the test specimens, respectively, according to the ASTM D790 standard. For each sample, at least three specimens are tested.

Interlaminar shear strength of discontinuous fiber composites is determined by short beam shear (SBS) testing following ASTM D2344 standard. Specimens with dimensions of 17.6 mm × 5.9 mm × 2.9 mm are prepared by printing and in-situ curing the composite ink (15 vol% carbon fibers) in parallel direction. Control samples are prepared by printing the ink in parallel direction in a silicone mold followed by curing at 170 °C for 1.5 h. Specimens are tested at a rate of 1 mm min^{-1}. At least three specimens are tested for each sample. Short beam shear strength is calculated as,

$$F = 0.75 \times \frac{P}{b \times h} \tag{4}$$

where P is the maximum observed load, b is the specimen width, and h is the specimen thickness.

Dynamic mechanical analysis experiments are conducted on printed and cast discontinuous fiber composite samples using a Dynamic Mechanical Analyzer (DMA, Q800 TA Instruments) in a dual cantilever mode. Thermal sweeps are performed from 30 °C to 250 °C at 3 °C min^{-1} at a constant frequency of 1 Hz and an amplitude of 20 µm. Rectangular bar specimens with dimensions of 60 mm × 12.7 mm × 3.2 mm are prepared for all samples. Glass transition temperature, T_g, is determined from the peak of the tan(δ) curve, and storage modulus, E', is recorded at 30 °C. Three specimens are tested for each sample.

Tensile tests on continuous fiber composites are performed on unidirectional printed and cast samples according to ASTM D3039 standard with a crosshead speed of 1.85 mm min^{-1} on a mechanical load frame (ATS Series 900) equipped with a 45 kN load cell. Tensile coupons are prepared with an overall length of 250 mm and a tab length of 52 mm using T700S carbon fibers (tow size = 12,000). For the preparation of printed samples, four layers, each with three rows of fiber tows, are printed and cured in-situ at a rate of 0.5 m min^{-1}. While printing the tensile bars, each layer is alternately shifted along the width by half the width of the tow to minimize void formation between layers. Control samples are prepared by placing fiber tows into a silicone mold sandwiched between two glass plates and cured at 170 °C for 1.5 h to create a 1-mm-thick composite panel. The panel is then cut into 10-mm wide test coupons. End tabs made from G10 FR4 glass fiber/epoxy sheets are adhered to specimens using a JB Weld adhesive. Five specimens are tested for each sample.

Optical microscopy

Optical microscopy is used to visually assess the quality of discontinuous and continuous FRPC parts, determine the orientation of fibers in discontinuous FRPCs, and measure the volume fraction of fibers in continuous FRPC parts. Microscopy specimens are cast in a mounting epoxy resin and polished using a polisher machine. Polished specimens are then imaged using a digital microscope (VHX-6000, Keyence). Fiber volume fraction is determined by calculating the total fiber area to cross-sectional area ratios using the Keyence microscope's built-in software. The circularity, C, of the cross-section of printed filaments is determined by calculating the ratio of the area of the filament cross-section, A, to the area of a circle with the same perimeter, P, as $C = 4\pi A/P^2$. The linearity of the discontinuous fiber-reinforced filament printed in midair in Fig. 2a is quantified by calculating the root mean square deviation (RMSD) of the printed path relative to the planned, straight-line path using the ImageJ software as,

$$RMSD = \sqrt{\frac{\sum_{i=1}^{N}(x_i - \hat{x}_i)^2}{N}} \tag{5}$$

where x_i and $\hat{x}_i$ respectively represent the actual path and the ideal line.

Data availability

Source data are provided with this paper. Any supplementary data that support the findings of this study are available from the corresponding author on request. Source data are provided with this paper.

References

1. Abliz, D. et al. Curing methods for advanced polymer composites - a review. *Polym. Polym. Compos.* **21**, 341–348 (2013).
2. Timmis, A. J. et al. Environmental impact assessment of aviation emission reduction through the implementation of composite materials. *Int. J. Life Cycle Assess.* **20**, 233–243 (2015).
3. Witik, R. A. et al. Economic and environmental assessment of alternative production methods for composite aircraft components. *J. Clean. Prod.* **29–30**, 91–102 (2012).
4. Li, Y., Xiao, Y., Yu, L., Ji, K. & Li, D. A review on the tooling technologies for composites manufacturing of aerospace structures: materials, structures and processes. *Compos., Part A* **154**, 106762 (2022).
5. CompositesWorld. The market for OOA aerocomposites, 2013-2022. *The market for OOA aerocomposites, 2013-2022* https://www.compositesworld.com/articles/the-market-for-ooa-aerocomposites-2013-2022 (2014).
6. Wong, J., Altassan, A. & Rosen, D. W. Additive manufacturing of fiber-reinforced polymer composites: A technical review and status of design methodologies. *Compos. Part B* **255**, 110603 (2023).
7. Gao, W. et al. The status, challenges, and future of additive manufacturing in engineering. *Comput. Aided Des.* **69**, 65–89 (2015).
8. van de Werken, N. et al. Additively manufactured carbon fiber-reinforced composites: State of the art and perspective. *Addit. Manuf.* **31**, 100962 (2020).
9. He, Q., Wang, H., Fu, K. & Ye, L. 3D printed continuous CF/PA6 composites: Effect of microscopic voids on mechanical performance. *Compos. Sci. Technol.* **191**, 108077 (2020).
10. Ueda, M. et al. 3D compaction printing of a continuous carbon fiber reinforced thermoplastic. *Compos. Part A* **137**, 105985 (2020).
11. Tu, R. & Sodano, H. A. Additive manufacturing of high-performance vinyl ester resin via direct ink writing with UV-thermal dual curing. *Addit. Manuf.* **46**, 102180 (2021).

12. Ji, Z., Jiang, D., Zhang, X., Guo, Y. & Wang, X. Facile photo and thermal two-stage curing for high-performance 3D printing of Poly(Dimethylsiloxane). *Macromol. Rapid Commun.* **41**, 2000064 (2020).
13. Maqsood, N. & Rimašauskas, M. Characterization of carbon fiber reinforced PLA composites manufactured by fused deposition modeling. *Compos. Part C.* **4**, 100112 (2021).
14. Bourgeois, M. E. & Radford, D. W. Digital manufacture of a continuous fiber reinforced thermoplastic matrix truss core structural panel using off-the-tool consolidation. *J. Compos. Sci.* **6**, 343 (2022).
15. Chang, B. et al. Additive manufacturing of continuous carbon fiber reinforced poly-ether-ether-ketone with ultrahigh mechanical properties. *Polym. Test.* **88**, 106563 (2020).
16. Li, S. et al. Advances in hybrid fibers reinforced polymer-based composites prepared by FDM: A review on mechanical properties and prospects. *Compos. Commun.* **40**, 101592 (2023).
17. Ferreira, R. T. L., Amatte, I. C., Dutra, T. A. & Bürger, D. Experimental characterization and micrography of 3D printed PLA and PLA reinforced with short carbon fibers. *Compos. Part B* **124**, 88–100 (2017).
18. Yang, D., Zhang, H., Wu, J. & McCarthy, E. D. Fibre flow and void formation in 3D printing of short-fibre reinforced thermoplastic composites: An experimental benchmark exercise. *Addit. Manuf.* **37**, 101686 (2021).
19. Sun, X., Mazur, M. & Cheng, C.-T. A review of void reduction strategies in material extrusion-based additive manufacturing. *Addit. Manuf.* **67**, 103463 (2023).
20. Blok, L. G., Longana, M. L., Yu, H. & Woods, B. K. S. An investigation into 3D printing of fibre reinforced thermoplastic composites. *Addit. Manuf.* **22**, 176–186 (2018).
21. Tekinalp, H. L. et al. Highly oriented carbon fiber–polymer composites via additive manufacturing. *Compos. Sci. Technol.* **105**, 144–150 (2014).
22. Guo, Y., Ji, Z., Zhang, Y., Wang, X. & Zhou, F. Solvent-free and photocurable polyimide inks for 3D printing. *J. Mater. Chem. A* **5**, 16307–16314 (2017).
23. Wu, T. et al. Additively manufacturing high-performance bismaleimide architectures with ultraviolet-assisted direct ink writing. *Mater. Des.* **180**, 107947 (2019).
24. Leguizamon, S. C., Cook, A. W. & Appelhans, L. N. Employing photosensitizers for rapid olefin metathesis additive manufacturing of Poly(dicyclopentadiene). *Chem. Mater.* **33**, 9677–9689 (2021).
25. Ming, Y., Xin, Z., Zhang, J., Duan, Y. & Wang, B. Fabrication of continuous glass fiber-reinforced dual-cure epoxy composites via UV-assisted fused deposition modeling. *Compos. Commun.* **21**, 100401 (2020).
26. Rahman, M. A., Islam, M. Z., Gibbon, L., Ulven, C. A. & La Scala, J. J. 3D printing of continuous carbon fiber reinforced thermoset composites using UV curable resin. *Polym. Compos.* **42**, 5859–5868 (2021).
27. Zhu, J., Zhang, Q., Yang, T., Liu, Y. & Liu, R. 3D printing of multi-scalable structures via high penetration near-infrared photopolymerization. *Nat. Commun.* **11**, 3462 (2020).
28. Baur, J. W. et al. Mechanical properties of additively printed, UV cured, continuous fiber unidirectional composites for multifunctional applications. *J. Compos. Mater.* **57**, 865–882 (2023).
29. Talley, S. J. et al. Impact of filler composition on mechanical and dynamic response of 3-D printed silicone-based nanocomposite elastomers. *Compos. Sci. Technol.* **198**, 108258 (2020).
30. Hmeidat, N. S., Kemp, J. W. & Compton, B. G. High-strength epoxy nanocomposites for 3D printing. *Compos. Sci. Technol.* **160**, 9–20 (2018).
31. Wang, B., Zhang, Z., Pei, Z., Qiu, J. & Wang, S. Current progress on the 3D printing of thermosets. *Adv. Compos. Hybrid. Mater.* **3**, 462–472 (2020).
32. Deng, K., Zhang, C., & Fu, K. Additive manufacturing of continuously reinforced thermally curable thermoset composites with rapid interlayer curing. *Compos. Part B: Eng.* **257**, 110671 (2023).
33. Compton, B. G. & Lewis, J. A. 3D-printing of lightweight cellular composites. *Adv. Mater.* **26**, 5930–5935 (2014).
34. Uitz, O., Koirala, P., Tehrani, M. & Seepersad, C. C. Fast, low-energy additive manufacturing of isotropic parts via reactive extrusion. *Addit. Manuf.* **41**, 101919 (2021).
35. Shi, B. et al. Dynamic capillary-driven additive manufacturing of continuous carbon fiber composite. *Matter* **2**, 1594–1604 (2020).
36. Ziaee, M., Johnson, J. W. & Yourdkhani, M. 3D printing of short-carbon-fiber-reinforced thermoset polymer composites via frontal polymerization. *ACS Appl. Mater. Interfaces* **14**, 16694–16702 (2022).
37. Zhang, Z. et al. Frontal polymerization-assisted 3D printing of short carbon fibers/dicyclopentadiene composites. *J. Manuf. Process.* **71**, 753–762 (2021).
38. Zhang, Z. et al. 3D printing of frontal-polymerized multiscale epoxy thermoset and composites. *Manuf. Lett.* **33**, 640–643 (2022).
39. Garg, M. et al. Rapid synchronized fabrication of vascularized thermosets and composites. *Nat. Commun.* **12**, 2836 (2021).
40. Aw, J. E. et al. Self-regulative direct ink writing of frontally polymerizing thermoset polymers. *Adv. Mater. Technol.* **7**, 2200230 (2022).
41. Ziaee, M., Naseri, I., Johnson, J. W., Franklin, K. A. & Yourdkhani, M. Frontal polymerization and three-dimensional printing of thermoset polymers with tunable thermomechanical properties. *ACS Appl. Polym. Mater.* **5**, 1715–1724 (2023).
42. Chen, Z., Ziaee, M., Yourdkhani, M. & Zhang, X. Multiphysics modeling of frontal polymerization-assisted layer-by-layer additive manufacturing of thermoset polymer components. *Addit. Manuf.* **59**, 103182 (2022).
43. Vallons, K. A. M., Drozdzak, R., Charret, M., Lomov, S. V. & Verpoest, I. Assessment of the mechanical behaviour of glass fibre composites with a tough polydicyclopentadiene (PDCPD) matrix. *Compos. Part A* **78**, 191–200 (2015).
44. Cheng, C. et al. Newly designed polydicyclopentadiene and its continuous carbon fiber composites: Preparation and mechanical properties assessment. *Polymer* **262**, 125481 (2022).
45. Hu, Y., Lang, A. W., Li, X. & Nutt, S. R. Hygrothermal aging effects on fatigue of glass fiber/polydicyclopentadiene composites. *Polym. Degrad. Stab.* **110**, 464–472 (2014).
46. Chang, K. M. et al. Durable and impact-resistant thermoset polymers for the extreme environment of low Earth orbit. *Extrem. Mech. Lett.* **64**, 102089 (2023).
47. Dean, L. M., Ravindra, A., Guo, A. X., Yourdkhani, M. & Sottos, N. R. Photothermal initiation of frontal polymerization using carbon nanoparticles. *ACS Appl. Polym. Mater.* **2**, 4690–4696 (2020).
48. Cook, A. L. et al. Polymer patterning by laser-induced multipoint initiation of frontal polymerization. *ACS Appl. Mater. Interfaces* **16**, 17973–17980 (2024).
49. Zhu, J. et al. Carbon materials for enhanced photothermal conversion: Preparation and applications on steam generation. *Mater. Rep.: Energy* **4**, 100245 (2024).
50. Robertson, I. D. et al. Rapid energy-efficient manufacturing of polymers and composites via frontal polymerization. *Nature* **557**, 223–227 (2018).
51. Robertson, I. D. et al. Alkyl phosphite inhibitors for frontal ring-opening metathesis polymerization greatly increase pot life. *ACS Macro Lett.* **6**, 609–612 (2017).
52. Ziaee, M. & Yourdkhani, M. Effect of resin staging on frontal polymerization of dicyclopentadiene. *J. Polym. Sci.* **59**, 1732–1739 (2021).
53. Ding, S. et al. Non-planar additive manufacturing of pre-impregnated continuous fiber reinforced composites using a three-axis printer. *J. Mater. Res. Technol.* **32**, 4410–4419 (2024).

54. Shang, J. et al. Z-direction performance and failure behavior of 3D printed continuous fiber reinforced composites with sinusoidal structure. *Compos. Sci. Technol.* **239**, 110069 (2023).
55. Lee, Y. B. et al. A self-healing system for polydicyclopentadiene thermosets. *Adv. Mater.* **36**, 2309662 (2024).
56. Zhang, Y., Huang, Z., Wang, H. & Li, J. Regulation of the interface compatibility of the 3D-printing interpenetration networks toward reduced structure anisotropy and enhanced performances. *ACS Appl. Mater. Interfaces* **15**, 32984–32992 (2023).
57. Wang, H., Huang, Z., Zhang, Y., Li, L. & Li, J. Design of enhanced mechanical properties by interpenetrating network of 3D printing dual-curing resins. *Polymer* **282**, 126153 (2023).

Acknowledgements

This work was primarily supported by the U.S. Department of Energy's Office of Energy Efficiency and Renewable Energy (EERE) under the Advanced Manufacturing Office, Award Number DE-EE0009404; supported in part by the National Science Foundation (NSF) Faculty Early Career Development Program, Award Number CMMI- 2239563; and supported in part by a proof-of-concept funding from the Colorado Office of Economic Development and International Trade, Award Number CTGGI 2020-2643. The authors thank Dr. James W. Johnson for conducting the flexural tests on composite specimens, Dr. Ravikumar Gowda for assistance in conducting DMA experiments on composite specimens, Patrick Baldwin and Sarah Danekind for their assistance with experiments, and Prof. Donald W. Radford for the helpful discussions. C.F.D. and M.Z. acknowledge summer internship awards from the Energy Institute at Colorado State University. The authors also thank the staff members of Colorado State University Analytical Resources Core Facility (RRID: SCR_021758) for their assistance with performing the DSC experiments.

Author contributions

M.Y. conceived the idea and directed the research. C.F.D., M.Z., A.M., and S.J.R. designed the experiments. M.Z. and C.F.D. performed most of the experiments and characterizations on discontinuous and continuous FRPCs, respectively. S.J.R. performed 3D printing of discontinuous FRPCs in Fig. 2i, j as well as the composite part containing aramid pulp (Fig. S4). A.M. focused on printing DMA samples and freeform printing of the bracket parts in Fig. 2k and Fig. 4j and their microscopy. All authors participated in writing or editing the manuscript.

Competing interests

The authors have been awarded the patent US11993018B2 related to this work.

Additional information

Supplementary information The online version contains supplementary material available at https://doi.org/10.1038/s41467-025-59848-2.

Correspondence and requests for materials should be addressed to Mostafa Yourdkhani.

Peer review information *Nature Communications* thanks the anonymous, reviewer(s) for their contribution to the peer review of this work. A peer review file is available.